

An Efficient Finite Element Formulation Based on Deformation Approach for Bending of Functionally Graded Beams

H. Ziou^{1,*}, M. Himeur², H. Guenfoud², M. Guenfoud²

¹National Centre of Integrated Studies and research on Building Engineering (CNERIB), Algeria

²LGCH Laboratory, University of Guelma, Algeria

Received 19 February 2020; accepted 10 April 2020

ABSTRACT

Finite element formulations based generally on classical beam theories such as Euler-Bernoulli or Timoshenko. Sometimes, these two formulations could be problematic expressed in terms of restrictions of Euler-Bernoulli beam theory, in case of thicker beams due to non-consideration of transverse shear; phenomenon that is known as shear locking characterized the Timoshenko beam theory, in case of thin beams; problem of slow of convergence in regards to the element of Timoshenko beam. In responding to this problematic, a new beam finite element model is developed to study the static bending of functionally graded beams. The originality of this model lies in the use of a deformation approach with the consideration of a central node positioned in the middle of the beam. The degrees of freedom of this node are subsequently eliminated by the method of static condensation. In addition, this model is suitable for all linear structures regardless of L/h ratio. Functionally graded material beams have a smooth variation of material properties due to continuous change in micro structural details. The mechanical properties of the beam are assumed to vary continuously in the thickness direction by a simple power-law distribution in terms of the volume fractions of the constituents. A simply supported beam subjected to uniform load for different length-to-thickness ratio has been chosen in the analysis. Finite element solutions obtained with the new finite element model are presented, and the obtained results are evaluated with the existing solutions to verify the validity of the present model.

© 2020 IAU, Arak Branch. All rights reserved.

Keywords: Deformation approach; Static condensation; Functionally graded beam; Finite element formulation.

1 INTRODUCTION

FUNCTIONALLY graded materials (FGMs) are a class of composite materials that have a gradual variation of material properties from one end to another. This gradual change of properties solves the weak points of layer

*Corresponding author. Tel.: +213 668598169.
E-mail address: hassina.geniecivil@gmail.com (H.Ziou).

composite materials (discontinuity of layers causes stress concentration and makes the layers susceptible for crack propagation, delimitation problem) and also provides very important capabilities for designers. FGM's find their applications in various fields such as the aerospace, aircraft, medicine, defense industries, automobile and most recently electronics sectors. Many studies for analysis of FGM beams, plates and shells are available in literatures.

A new beam element based on the first order shear deformation theory was developed to study the thermo elastic behavior of FGM beam structures by Chakraborty and Gopalakrishnan [1]. Kadoli et al. [2] proposed a fined element based on a third-order approximation of the axial displacement and constant transverse displacement for the static analysis of beams made of metal-ceramic FGMs. Components' volume fraction was supposed to vary according to a power-law function. A discrete layer approach was adopted to account for material gradation. Kapuria et al. [3] presented a finite element model for static and free vibration responses of layered FG beams using an efficient third order zigzag theory for estimating the effective modulus of elasticity, and its experimental validation for two different FGM systems under various boundary conditions. Pindera and Dunn [4] evaluated the higher order theory by performing a detailed finite element analysis of the FGM. They found that the HOTFGM results agreed well with the FE results. Ziou et al. [5] developed an exact element based on the first order shear deformation theory, a cantilever beam subjected to a concentrated force at the free end for different length-to-thickness ratio has been chosen for the analysis. The influences of the volume fraction index, length-to-thickness ratio and the Poisson's ratio on the mid plane deflections, stresses distribution and strain energy along the thickness of FGM beam are examined. It has been confirmed also with an energetic method that no significant variation on deformation with respect to variation in Poisson ratio. Nguyen and Gan [6] studied the large deflections of tapered functionally graded beams subjected to end forces by using the finite element method. Nguyen [7] is investigated by the FEM the large displacement response of tapered cantilever beams made of axially FGM. Kutiš et al. [8] presented a finite element procedure for modelling a FGM beam with spatial variation of material properties. Murin and Kutiš [9] introduced a new 3D-beam Euler-Bernoulli finite element for an analysis of beams with an arbitrary continuous smoothly varying cross section. A new higher order shear deformation model is developed for static and free vibration analysis of functionally graded beams by Lazreg et al. [10] with considering porosities that may possibly occur inside the functionally graded materials (FGMs) during their fabrication. Various micromechanical models are used to evaluate the mechanical characteristics of the FG beams whose properties vary continuously across the thickness according to a simple power law, after that they compared the presented results with the existing solutions available in the literature. The static behavior of non-prismatic sandwich beams composed of functionally graded (FG) materials was first investigated by Rezaiee-Pajand [11]. A new sinusoidal shear deformation theory based on the neutral surface concept was developed to study the static analysis of simply supported functionally graded plate by Benferhat et al. [12], the shear correction factor is not necessary in this study. Lazreg et al. [13] proposed a new first shear deformation plate theory based on neutral surface position for the static and the free vibration analysis of plates made of metal-ceramic FGMs. The mechanical properties of the plate are assumed to vary continuously in the thickness direction by a simple power-law distribution in terms of the volume fractions of the constituents. They found that the presented results agreed well with the existing solutions. Guenfoud et al. [14] developed a consistent triangular thin flat shell finite element based on strain approach, they considered that the geometry of shells can be approached by superimposing a membrane element and a plate element. The performance and efficiency of this model were evaluated through validation tests. Alshorbagy et al. [15] presented the dynamic characteristics of FGM beam with axial and transversal variation of material properties based on the power law, Eltaher et al. [16,17] studied static, stability and free vibration behaviors of FGM size-dependent nano-beams using finite element model, by using the model of Eringen. Mahmoud et al. [18] investigated a nonlocal bending behavior of nano-sized Euler-Bernoulli beam including surface effects. The surface layer is assumed elastic and isotropic, Gurtin-Murdoch's theory is employed. The vibration characteristics of both nonlinear symmetric power and sigmoid functionally graded nonlocal Nano beams was developed by Hamed et al. [19]. The most cited references are based on the displacement approach. Therefore, based on the above discussion there is a strong encouragement to understand the mechanical behavior of FGM beams but in another way by using another approaches.

In the present paper, a new finite element formulation is developed to study the static bending of functionally graded beams. The novelty of this formulation is the use of a deformation approach and consideration of a central node located in the barycenter of the beam. The degrees of freedom of this node are subsequently eliminated by the method of static condensation. The material constituents of beams assumed to be varying through the thickness direction according to a simple power law. The model has been verified with the existing solutions and found a good agreement with them. Numerical results are presented in both tabular and graphical forms to figure out the effects of different slenderness ratios and material distribution, on the static analysis.

2 MATERIAL PROPERTIES OF FGM BEAM

Fig.1 shows a FGM beam composed of ceramic and metal of length L , width b and thickness h . Material properties vary continuously and non-uniformly in the z direction.



Fig.1
Geometry of FGM beam and the possible variation of ceramic and metal through thickness.

Topmost surface consists of only ceramic and bottom surface has only metal. In between volume fraction of ceramic V_c and metal V_m are obtained by power law distribution in conjunction with simple law of constituent mixture as follows:

$$V_c = \left(\frac{z}{h} + \frac{1}{2} \right)^p \tag{1a}$$

$$V_m = 1 - V_c \tag{1b}$$

where, p is the power law index, a non-negative variable parameter which dictates the material variation profile through the thickness of the FGM beam. For $p = 0$ volume fraction of ceramic becomes one and homogeneous beam consisting only ceramic is obtained, when value of p is increased, content of metal in FGM increases.

It is assumed that material properties of the beam, such as Young's modulus (E) and mass density (ρ) vary continuously through the beam thickness according to power-law form, which can be described by

$$MP_{eff} = MP_m V_m(z) + MP_c V_c(z) \tag{2}$$

where, MP_m and MP_c stands for material properties of metals and ceramics respectively. Thus, the modulus of elasticity E_{eff} , Poisson's ratio ν_{eff} and shear modulus G_{eff} , of FGMs can be given by

$$E_{eff} = (E_c - E_m) \left(\frac{z}{h} + \frac{1}{2} \right)^p + E_m \tag{3a}$$

$$\nu_{eff} = (\nu_c - \nu_m) \left(\frac{z}{h} + \frac{1}{2} \right)^p + \nu_m \tag{3b}$$

$$G_{eff} = (G_c - G_m) \left(\frac{z}{h} + \frac{1}{2} \right)^p + G_m \tag{3c}$$

3 FINITE ELEMENT FORMULATION

3.1 Kinematic

By considering a straight beam of length L and axis x linking the gravity center G of all cross-sections with xz being a principal plane of inertia. The axial and vertical displacements of a point A of the beam section are expressed as:

$$u(x, z) = u_0(x) - z \phi(x) \tag{4a}$$

$$w(x, z) = w_0(x) \tag{4b}$$

where $(-)_0$ denotes the displacements of the beams axis.

The axial and transverse strains are deduced from Eqs. (4) as:

$$\varepsilon_{xx} = \frac{\partial u_0}{\partial x} - z \frac{\partial \phi}{\partial x} = \varepsilon_{xx}^0 - z \kappa_{xx}^0 \quad (5a)$$

$$\gamma_{xz} = \frac{\partial w_0}{\partial x} - \phi \quad (5b)$$

Eq. (5) can be written in matrix form as:

$$\varepsilon = \begin{Bmatrix} \varepsilon_x \\ \gamma_{xz} \end{Bmatrix} = \begin{bmatrix} 1 & -z & 0 \\ 0 & 0 & 1 \end{bmatrix} \begin{bmatrix} \frac{\partial u_0}{\partial x} & \frac{\partial \phi}{\partial x} & \frac{\partial w_0}{\partial x} - \phi \end{bmatrix}^T = S \hat{\varepsilon} \quad (6)$$

where ε is the strain vector, $\hat{\varepsilon}$ is the generalized strain vector containing the elongation of the beam axis $\frac{\partial u_0}{\partial x}$, the curvature $\frac{\partial \phi}{\partial x}$ and the transverse shear strain $\frac{\partial w_0}{\partial x} - \phi$ and S is a strain-displacement transformation matrix depending on the thickness coordinate z .

3.2 Stresses and results stresses

The axial and shear stresses are expressed from Eq. (5) as:

$$\sigma_x = E(z) \varepsilon_x = E(z) \left(\frac{\partial u_0}{\partial x} - z \frac{\partial \phi}{\partial x} \right) = \sigma_x^n(x) + \sigma_x^p(x) \quad (7a)$$

$$\tau_{xz} = G(z) \gamma_{xz} = G(z) \left(\frac{\partial w_0}{\partial x} - \phi \right) = \frac{E(z)}{2(1+\nu)} \left(\frac{\partial w_0}{\partial x} - \phi \right) \quad (7b)$$

where $E = E(x; z)$ and $G = G(x; z)$ are the longitudinal Young modulus and the shear modulus of the FGM beam.

$\sigma_x^n(x) = E(z) \frac{\partial u_0}{\partial x}$: Normal stress generated by forces along the axis of the beam.

$\sigma_x^p(x) = -zE(z) \frac{\partial \phi}{\partial x}$: Normal stress generated by forces in the plane of the beam.

Eq. (7) can be written in matrix form using Eq. (6a) as:

$$\sigma = \begin{Bmatrix} \sigma_x \\ \tau_{xz} \end{Bmatrix} = \begin{bmatrix} E(z) & 0 \\ 0 & G(z) \end{bmatrix} \begin{Bmatrix} \varepsilon_x \\ \gamma_{xz} \end{Bmatrix} = D \varepsilon = DS \hat{\varepsilon} \quad (8)$$

where D is the standard constitutive matrix relating stresses and strains at a point in the transverse cross section.

The axial force N , the bending moment M and the shear force Q in a beam section are obtained as:

$$\hat{\sigma} = \begin{Bmatrix} N \\ M \\ Q \end{Bmatrix} = \iint \begin{Bmatrix} \sigma_x \\ -z \sigma_x \\ \tau_{xz} \end{Bmatrix} dA = \iint S^T \sigma dA \quad (9)$$

where $\hat{\sigma}$ is the resultant stress vector and A is the area of the cross-section.

For an unloaded FGM beam with constant section, the two equilibrium equations are

$$\frac{\partial}{\partial x} \left(\frac{\partial w_0}{\partial x} - \phi \right) = 0 \tag{10a}$$

$$\frac{\partial^2 \phi}{\partial x^2} \hat{D}_b + G(z) A \kappa_z \left(\frac{\partial w_0}{\partial x} - \phi \right) = 0 \tag{10b}$$

$$\begin{cases} \hat{D}_a = b \int_{-h/2}^{+h/2} E(z) dz \\ \hat{D}_b = b \int_{-h/2}^{+h/2} E(z) z^2 dz \\ \hat{D}_{ab} = b \int_{-h/2}^{+h/2} E(z) z dz \end{cases} \tag{10c}$$

where b is the width of the beam. \hat{D}_a is the axial stiffness \hat{D}_b is the bending stiffness, \hat{D}_{ab} is the coupling axial-bending stiffness.

3.3 Structure of the beam 3_MS element

The beam element "Beam_3_MS" is a linear element with three nodes, the third one located in the barycenter of the element as shown in Fig. 2. Each node "i" has three degrees of freedom u_{0i} , ϕ_i and w_i .

Thus, it is an element with two independent transformation functions:

- Fields induced by the membrane behaviour whose interpolation polynomials have 03 parameters: α_1 , α_2 and α_3 .
- Fields induced by the flexional behaviour whose interpolation polynomials have 06 parameters: a_1 , a_2 , a_3 , a_4 , a_5 and a_6 .

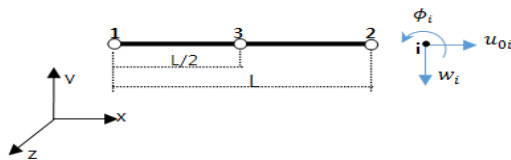


Fig.2 Structure of the "Beam_3_MS" beam element.

3.3.1 Fields of transformations and shape functions

The process based upon the deformation approach implies the use of the interpolation parameters to describe the deformation field. In addition, the displacement field is obtained by integrating the corresponding deformation.

a. Membrane behavior

$$\begin{cases} \varepsilon_{0xx}(x) = \frac{\partial u_0(x)}{\partial x} \\ u_0(x) = \int \varepsilon_{0xx}(x) \partial x \end{cases} \tag{11}$$

Thus, for rigid body movements (RBM), deformation is null

$$\varepsilon_{0xx}(x) = \frac{\partial u_0(x)}{\partial x} = 0 \tag{12}$$

Integrating Eq. (12) yields

$$u_{0RBM}(x) = \alpha_1 \quad (13)$$

For the other modes, the axial deformation field has a polynomial form, it constructed around the remaining parameters α_2 and α_3 .

$$\varepsilon_{0AMxx}(x) = \alpha_2 + \alpha_3 x \quad (14)$$

Integrating Eq. (14), we obtain the axial displacement field for the other modes as:

$$u_{0AM}(x) = \alpha_2 x + \alpha_3 \frac{x^2}{2} \quad (15)$$

In matrix form, the final fields are written, as follows:

$$u_0(x) = \left\langle 1 \quad x \quad \frac{x^2}{2} \right\rangle \begin{Bmatrix} \alpha_1 \\ \alpha_2 \\ \alpha_3 \end{Bmatrix} \quad (16)$$

$$\varepsilon_{0xx}(x) = \langle 0 \quad 1 \quad x \rangle \begin{Bmatrix} \alpha_1 \\ \alpha_2 \\ \alpha_3 \end{Bmatrix} \quad (17)$$

For a beam of length L , the nodal displacements vector is given as follows:

$$\begin{Bmatrix} u_{01} \\ u_{02} \\ u_{03} \end{Bmatrix} = \begin{bmatrix} 1 & 0 & 0 \\ 1 & L & \frac{L^2}{2} \\ 1 & \frac{L}{2} & \frac{L^2}{8} \end{bmatrix} \begin{Bmatrix} \alpha_1 \\ \alpha_2 \\ \alpha_3 \end{Bmatrix} \quad (18)$$

The expression of the interpolation parameters is given as a function of the nodal displacements

$$\begin{Bmatrix} \alpha_1 \\ \alpha_2 \\ \alpha_3 \end{Bmatrix} = \begin{bmatrix} 1 & 0 & 0 \\ 1 & L & \frac{L^2}{2} \\ 1 & \frac{L}{2} & \frac{L^2}{8} \end{bmatrix}^{-1} \begin{Bmatrix} u_{01} \\ u_{02} \\ u_{03} \end{Bmatrix} = \frac{1}{L^2} \begin{bmatrix} L^2 & 0 & 0 \\ -3L & -L & 4L \\ 4 & 4 & -8 \end{bmatrix} \begin{Bmatrix} u_{01} \\ u_{02} \\ u_{03} \end{Bmatrix} \quad (19)$$

Eqs. (16) and (17) are respectively, the displacements fields and the deformations fields defined as:

$$u_0(x) = \left\langle 1 \quad x \quad \frac{x^2}{2} \right\rangle \frac{1}{L^2} \begin{bmatrix} L^2 & 0 & 0 \\ -3L & -L & 4L \\ 4 & 4 & -8 \end{bmatrix} \begin{Bmatrix} u_{01} \\ u_{02} \\ u_{03} \end{Bmatrix} \quad (20)$$

$$\varepsilon_{0xx}(x) = \langle 0 \quad 1 \quad x \rangle \frac{1}{L^2} \begin{bmatrix} L^2 & 0 & 0 \\ -3L & -L & 4L \\ 4 & 4 & -8 \end{bmatrix} \begin{Bmatrix} u_{01} \\ u_{02} \\ u_{03} \end{Bmatrix} \quad (21)$$

The shape functions describing the membrane behaviour can be obtained as following

$$\langle Nu_{01}(x) \quad Nu_{02}(x) \quad Nu_{03}(x) \rangle = \left\langle 1 \quad x \quad \frac{x^2}{2} \right\rangle \frac{1}{L^2} \begin{bmatrix} L^2 & 0 & 0 \\ -3L & -L & 4L \\ 4 & 4 & -8 \end{bmatrix} \quad (22)$$

Hence,

$$\begin{cases} Nu_{01}(x) = \frac{1}{L^2}(L^2 - 3Lx + 2x^2) \\ Nu_{02}(x) = \frac{1}{L^2}(-Lx + 2x^2) \\ Nu_{03}(x) = \frac{1}{L^2}(4Lx - 4x^2) \end{cases} \quad (23)$$

$$\begin{cases} N'u_{01}(x) = \frac{1}{L^2}(-3L + 4x) \\ N'u_{02}(x) = \frac{1}{L^2}(-L + 4x) \\ N'u_{03}(x) = \frac{1}{L^2}(4L - 8x) \end{cases} \quad (24)$$

b. Flexional behavior

The only nonzero strain is given by

$$\begin{cases} \varepsilon_{fxx}(x) = -z \frac{\partial \phi}{\partial x} \\ \gamma_{xz} = \frac{\partial w_0}{\partial x} - \phi \end{cases} \quad (25)$$

Deformations are null for the Rigid Body Movements (RBM),

$$\begin{cases} \varepsilon_{fxx}(x) = -z \frac{\partial \phi}{\partial x} = 0 \\ \gamma_{xz} = \frac{\partial w_0}{\partial x} - \phi = 0 \end{cases} \quad (26)$$

By integrating Eq. (26), we obtain the displacement field of rigid body mode

$$\begin{Bmatrix} w_0 \\ \phi \end{Bmatrix}_{RBM} = \frac{1}{z} \begin{bmatrix} 1 & x \\ 0 & 1 \end{bmatrix} \begin{Bmatrix} a_1 \\ a_2 \end{Bmatrix} \quad (27)$$

Always the deformation field has a polynomial form for the other modes. It constructed around the remaining parameters a_3, a_4, a_5 and a_6 and satisfying the equilibrium conditions given in Eqs. (10).

$$\begin{cases} \varepsilon_{fxx}(x) \\ \gamma_{xz}(x) \end{cases}_{AM} = \begin{bmatrix} -1 & -2x & (-3x^2 + 6\alpha) & (-4x^3 + 18\alpha x) \\ 0 & -\alpha & 0 & 0 \end{bmatrix} \begin{Bmatrix} a_1 \\ a_2 \\ a_3 \\ a_4 \end{Bmatrix} \quad (28)$$

$$\alpha = \frac{\int_{-h/2}^{+h/2} E(z) z^2 dz}{\kappa_z \int_{-h/2}^{+h/2} G(z) dz}$$

After integrating Eq. (28), the displacement field for the other modes is expressed as:

$$\begin{cases} w_0(x) \\ \phi(x) \end{cases}_{AM} = \frac{1}{z} \begin{bmatrix} \frac{x^2}{2} \left(\frac{x^3}{3} - \alpha x \right) \left(\frac{x^4}{4} - 3\alpha x^2 \right) \left(\frac{x^5}{5} - 3\alpha x^3 \right) \\ x & x^2 & (x^3 - 6\alpha x) & (x^4 - 9\alpha x^2) \end{bmatrix} \begin{Bmatrix} a_1 \\ a_2 \\ a_3 \\ a_4 \end{Bmatrix} \quad (29)$$

The final fields has the following matrix form

$$\begin{cases} w_0(x) \\ \phi(x) \end{cases}_{AM} = \frac{1}{z} \begin{bmatrix} 1 & x & \frac{x^2}{2} \left(\frac{x^3}{3} - \alpha x \right) \left(\frac{x^4}{4} - 3\alpha x^2 \right) \left(\frac{x^5}{5} - 3\alpha x^3 \right) \\ 0 & 1 & x & x^2 & (x^3 - 6\alpha x) & (x^4 - 9\alpha x^2) \end{bmatrix} \begin{Bmatrix} a_1 \\ a_2 \\ a_3 \\ a_4 \\ a_5 \\ a_6 \end{Bmatrix} \quad (30)$$

$$\begin{cases} \varepsilon_{fxx}(x) \\ \gamma_{xz}(x) \end{cases} = \frac{1}{z} \begin{bmatrix} 0 & 0 & -1 & -2x & (-3x^2 + 6\alpha) & (-4x^3 + 18\alpha x) \\ 0 & 0 & 0 & -\alpha & 0 & 0 \end{bmatrix} \begin{Bmatrix} a_1 \\ a_2 \\ a_3 \\ a_4 \\ a_5 \\ a_6 \end{Bmatrix} \quad (31)$$

For a beam of length L , the nodal displacements vector can be written as:

$$\begin{cases} w_{01} \\ \phi_1 \\ w_{02} \\ \phi_2 \\ w_{03} \\ \phi_3 \end{cases} = \frac{1}{z} \begin{bmatrix} 1 & 0 & 0 & 0 & 0 & 0 \\ 0 & 1 & 0 & 0 & 0 & 0 \\ 1 & L & \frac{L^2}{2} \left(\frac{L^3}{3} - \alpha L \right) \left(\frac{L^4}{4} - 3\alpha L^2 \right) \left(\frac{L^5}{5} - 3\alpha L^3 \right) \\ 0 & 1 & L & L^2 & L^3 - 6\alpha L & L^4 - 9\alpha L^2 \\ 1 & \frac{L}{2} & \frac{L^2}{8} \left(\frac{L^3}{24} - \alpha \frac{L}{2} \right) \left(\frac{L^4}{64} - 3\alpha \frac{L^2}{4} \right) \left(\frac{L^5}{160} - 3\alpha \frac{L^3}{8} \right) \\ 0 & 1 & \frac{L}{2} & \frac{L^2}{4} & \frac{L^3}{8} - 3\alpha L & \left(\frac{L^4}{16} - 9\alpha \frac{L^2}{4} \right) \end{bmatrix} \begin{Bmatrix} a_1 \\ a_2 \\ a_3 \\ a_4 \\ a_5 \\ a_6 \end{Bmatrix} \quad (32)$$

Eq. (32) can be rewritten as:

$$\begin{Bmatrix} w_{01} \\ \phi_1 \\ w_{02} \\ \phi_2 \\ w_{03} \\ \phi_3 \end{Bmatrix} = \frac{1}{z} [A] \begin{Bmatrix} a_1 \\ a_2 \\ a_3 \\ a_4 \\ a_5 \\ a_6 \end{Bmatrix} \tag{33}$$

[A] is the nodal coordinate matrix which is given in Eq. (32). The expression of the given interpolation parameters as a function of the nodal displacements is given by

$$\begin{Bmatrix} a_1 \\ a_2 \\ a_3 \\ a_4 \\ a_5 \\ a_6 \end{Bmatrix} = z [A]^{-1} \begin{Bmatrix} w_{01} \\ \phi_1 \\ w_{02} \\ \phi_2 \\ w_{03} \\ \phi_3 \end{Bmatrix} \tag{34}$$

Eqs. (30) and (31) are respectively the corresponding displacements fields and the deformations fields,

$$\begin{Bmatrix} w_0(x) \\ \phi(x) \end{Bmatrix} = \begin{bmatrix} 1 & x & \frac{x^2}{2} \left(\frac{x^3}{3} - \alpha x \right) & \left(\frac{x^4}{4} - 3\alpha x^2 \right) & \left(\frac{x^5}{5} - 3\alpha x^3 \right) \\ 0 & 1 & x & x^2 & (x^3 - 6\alpha x) & (x^4 - 9\alpha x^2) \end{bmatrix} [A]^{-1} \begin{Bmatrix} w_{01} \\ \phi_1 \\ w_{02} \\ \phi_2 \\ w_{03} \\ \phi_3 \end{Bmatrix} \tag{35}$$

$$\begin{Bmatrix} \varepsilon_{xx}(x) \\ \gamma_{xz}(x) \end{Bmatrix} = \begin{bmatrix} 0 & 0 & -1 - 2x & (-3x^2 + 6\alpha) & (-4x^3 + 18\alpha x) \\ 0 & 0 & 0 & -\alpha & 0 \end{bmatrix} [A]^{-1} \begin{Bmatrix} w_{01} \\ \phi_1 \\ w_{02} \\ \phi_2 \\ w_{03} \\ \phi_3 \end{Bmatrix} \tag{36}$$

The right hand side of Eq. (32) represents the shape functions, $\langle N_1(x) N_2(x) N_3(x) N_4(x) N_5(x) N_6(x) \rangle$, with a higher degree of interpolation. In addition, the right hand side of Eq. (33) represents the deformation matrix.

3.4 Stiffness matrix

The stiffness matrix can be divided into sub-matrices as follows:

- Membrane rigidity

The stiffness matrix is obtained from the elementary virtual work, given by this expression

$$(\delta W_{int})^e = \int_{V^e} \delta \{ \varepsilon_{xx}^0(x) \}^T [\sigma_x^n(x)] dV^e = \delta \{ q^e \}^T b \int_{-h/2}^{+h/2} E(z) dz \int_0^L [B^m]^T [B^m] dx \{ q^e \} \tag{37}$$

$\{ q^e \}^T = \langle u_{01} \quad u_{02} \quad u_{03} \rangle$ is the nodal displacements vector.

The elementary stiffness matrix, before static condensation, can be written as:

$$[K_{NC}^m]^e = b \int_{-h/2}^{+h/2} E(z) dz \int_0^L [B^m]^T [B^m] dx \quad (38)$$

where $[B^m] = [N'u_{01}(x) \quad N'u_{02}(x) \quad N'u_{03}(x)] = \left[\frac{1}{L^2}(-3L+4x) \quad \frac{1}{L^2}(-L+4x) \quad \frac{1}{L^2}(4L-8x) \right]$

After few manipulations, we obtain

$$[K_{NC}^m]^e = \frac{\hat{D}_a}{3L} \begin{bmatrix} 7 & 1 & -8 \\ 1 & 7 & -8 \\ -8 & -8 & 16 \end{bmatrix} \quad (39)$$

The elementary stiffness matrix after static condensation is defined as:

$$[K_C^m]^e = \frac{\hat{D}_a}{L} \begin{bmatrix} 1 & -1 \\ -1 & 1 \end{bmatrix} \quad (40)$$

- Flexural and shear rigidity

The stiffness matrix of the bending behaviour is obtained from the discretized elementary virtual work, given by the following expression

$$(\delta \mathcal{W}_{int})^e = \int_{V^e} \delta \left\{ \begin{matrix} \kappa_{xx}^0(x) \\ \gamma_{xy}(x) \end{matrix} \right\}^T \left[\begin{matrix} \sigma_x^p(x) \\ \tau_{xy} \end{matrix} \right] dV^e = \delta \{q^e\}^T \int_0^L [B^f]^T \begin{bmatrix} E(z) & 0 \\ 0 & G(z) \end{bmatrix} [B^f] dV^e \{q^e\} \quad (41)$$

$\{q^e\}^T = \langle v_1 \quad \theta_{z_1} \quad v_2 \quad \theta_{z_2} \quad v_3 \quad \theta_{z_3} \rangle$ is the vector of nodal displacements.

Before static condensation, we get the following elementary stiffness matrix

$$[K_{NC}^f]^e = \int_0^L [B^f]^T \begin{bmatrix} E(z) & 0 \\ 0 & G(z) \end{bmatrix} [B^f] dV^e = b \int_{-h/2}^{+h/2} z^2 E(z) dz [A^{-1}]^T \left(\int_0^L [Q(x)^f]^T \begin{bmatrix} 1 & 0 \\ 0 & \frac{1}{\alpha} \end{bmatrix} [Q(x)^f] dx \right) [A^{-1}] \quad (42)$$

where

$$[Q(x)^f] = \begin{bmatrix} 0 & 0 & -1 & -2x & (-3x^2+6\alpha) & (-4x^3+18\alpha x) \\ 0 & 0 & 0 & -\alpha & 0 & 0 \end{bmatrix}$$

$$[K^0]^e = \int_0^L [Q(x)^f]^T \begin{bmatrix} 1 & 0 \\ 0 & \frac{1}{\alpha} \end{bmatrix} [Q(x)^f] dx$$

Eq. (42) can be simplified as follows:

$$[K_{NC}^f]^e = \hat{D}_b [A^{-1}]^T [K^0]^e [A^{-1}] \quad (43)$$

- Coupling rigidity

The virtual work done by a stress field σ on a virtual strain field ε can be represented by

$$(\delta W_{int})^e = \int_{V^e} \delta \{ \varepsilon_m \}^T [\sigma_f] dV^e \tag{44}$$

Knowing that

$$\{ \varepsilon_m \} = [Q(x)^m] [A_m]^{-1} \{ q_m^e \} \tag{45a}$$

$$\{ \sigma_f \} = b \int_{-h/2}^{+h/2} E(z) z dz \{ \varepsilon_f \} \tag{45b}$$

By substituting Eqs. (45a) and (45b) into (44) yields

$$(\delta W_{int})^e = \delta \{ q_m^e \}^T \times \int_0^L [Q(x)^m]^T [A_m^{-1}]^T \times b \int_{-h/2}^{+h/2} E(z) z dz \times [Q(x)^f] [A_f]^{-1} \{ q_f \} dx \tag{46}$$

The elementary stiffness matrix, from the expression (46) can be written as:

$$[K_c^e] = \int_0^L [Q(x)^m]^T [A_m^{-1}]^T \times b \int_{-h/2}^{+h/2} E(z) z dz \times [Q(x)^f] [A_f]^{-1} dx \tag{47}$$

or

$$[K_c^e] = [A_m^{-1}]^T \int_0^L [Q(x)^m]^T \times \hat{D}_{ab} \times [Q(x)^f] dx [A_f]^{-1} = [A_m^{-1}]^T [K_0^c] [A_f]^{-1} \tag{48}$$

The evaluation of the expression $[K_0^c]^e$ and $[K_c^e]^e$ are established by analytical integration of the different components resulting from the matrix product $b \int_{-h/2}^{+h/2} E(z) z^2 dz \times [Q(x)^f]^T \begin{bmatrix} 1 & 0 \\ 0 & \frac{1}{\alpha} \end{bmatrix} [Q(x)^f]$ and $b \int_{-h/2}^{+h/2} E(z) z dz \times [Q_m]^T [Q_f]$ respectively. Which are defined in Appendix.

4 NUMERICAL RESULTS AND DISCUSSIONS

In order to demonstrate the efficiency of the present approach (deformation approach), various numerical examples are presented and discussed, after that the present results are compared with the data available in literature. For this purpose of verification, An Al/Al₂O₃ beam composed of aluminum (metal) and alumina (ceramic) is considered. The material properties of aluminum are: $E_m = 70GPa$, $\nu_m = 0.3$. And those of alumina are $E_m = 380GPa$, $\nu_m = 0.3$.

The non-dimensional quantities used in the present analysis are defined as:

$$\bar{w} = 100 \frac{E_m h^3}{qL^4} w \left(\frac{L}{2} \right), \bar{\sigma}_{xx} = \frac{h}{qL} \sigma_x \left(\frac{L}{2}, \frac{h}{2} \right), \bar{\sigma}_{xz} = \frac{h}{qL} \sigma_{xz} (0,0)$$

Non-dimensional deflections and stresses of FGM beams under uniform load for different power law index and different length-to-thickness ratio are given in Table 1. The calculated values based on the present approach are obtained, it can be observed that the values obtained using the deformation approach are in good agreement with those given by Li et al. [20] for all values of power law index and length-to-thickness ratio.

It is worth noting that the values of Li et al. [20] are calculated based on the analytical solutions (see Appendix in the Ref Li et al. [20]).

Table 1

Non-dimensional deflections and normal stresses of FGM beams under uniform load. The material properties of glass fiber and ester resin matrix.

L/h	p	\bar{w}		$\bar{\sigma}_{xx}$		$\bar{\sigma}_{xz}$	
		Li et al. [20]	Present	Li et al. [20]	Present	Li et al. [20]	Present
5	0	31.65	31.66	38.02	37.60	7.50	7.50
	1	62.59	62.55	58.83	58.13	7.50	7.51
	2	80.60	80.19	68.81	67.88	6.78	6.38
	5	97.80	96.33	81.03	79.67	5.79	5.12
20	0	28.96	29.01	150.13	150.41	7.50	7.50
	1	58.04	58.09	232.05	232.57	7.50	7.51
	2	74.41	74.40	270.98	271.52	6.78	6.38
	5	88.15	88.06	318.11	318.66	5.79	5.12

To depict the effect of the power law index on the bending response of FGM beams, non-dimensional transverse deflection, and axial normal stress are plotted in Fig. 3. The present approach is used only in these figures. As expected, the increasing of power law index leads to an increase in the deflection and axial stress, this is due to the fact that an increase in power law index p results in a decrease in the value of elasticity modulus, and thus makes FGM beams more flexible. It is cleared shown also that the highest values of transverse deflection and axial normal stress are obtained for full metal beams ($p \rightarrow \infty$), while the lowest values are obtained for full ceramic beams ($p=0$).

Fig. 4 depicts the variation of the non-dimensional shear stress across the thickness of FGM beam under uniform load, with the present approach at $x=0$. The power law index p of the FGM beam shifted from 0 to 5. With increasing of the power law index, the tip of shear stress increases. The maximum value of shear stress occurs at the neutral axis not at mid-plane unless for an isotropic beam.

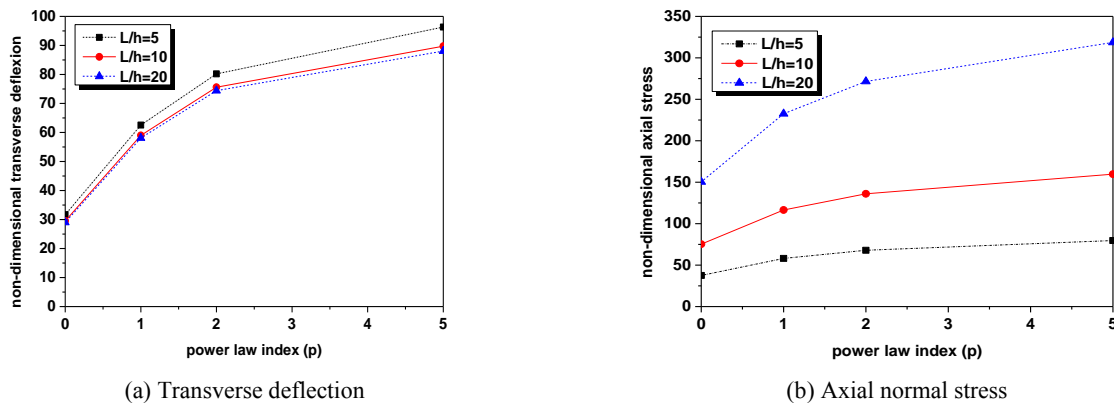


Fig.3

Variation of non-dimensional transverse deflection and axial normal stress with respect to the power law index for FGM beams under uniform load.

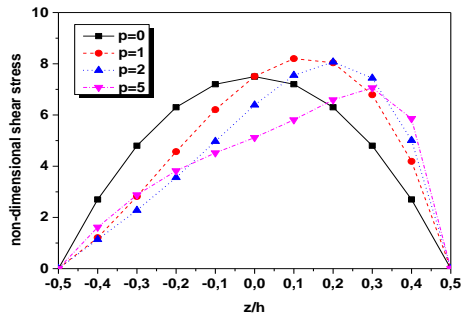


Fig.4 Depthwise shear stresses distribution under uniform load q at $x = 0$.

5 CONCLUSION

In this paper, a finite element procedure for static analysis of functionally graded material (FGM) beam is presented. The novelty of this procedure is the use of a deformation approach and consideration of a central node positioned in the middle of the beam. The degrees of freedom of this node are subsequently eliminated by the method of static condensation. The present approach, the development concepts and the techniques used in this paper allowed us to obtain competitive, robust and efficient finite element model to treat both thin and thick linear structures whatever L/h ratio. The material properties of the beam are assumed to vary continuously along the beam thickness by a power-law distribution. A FORTRAN code is constructed to compute to predict the static responses. A simply supported beam subjected to uniform load for different length-to-thickness ratio has been chosen. The influences of material composition and aspect ratio on the mid plane deflections, normal stress and shear stress distributions along the thickness of the beam are examined and highlighted. The obtained results are compared with the data available in the literature using analytical solutions to verify the validity of the developed model.

APPENDIX

The elementary stiffness matrix before condensation (flexural and shear rigidity)

$$[K_{NC}^f]^e = \int_0^L [B^f]^{-T} \begin{bmatrix} E(z) & 0 \\ 0 & G(z) \end{bmatrix} [B^f] dV^e = [A^{-1}]^T \left(b \int_{-h/2}^{+h/2} z^2 E(z) dz \times \int_0^L [Q(x)^f]^T \begin{bmatrix} 1 & 0 \\ 0 & \frac{1}{\alpha} \end{bmatrix} [Q(x)^f] dx \right) [A^{-1}]$$

Where

$$[K^0]^e = \hat{D}_b \times \int_0^L [Q(x)^f]^T \begin{bmatrix} 1 & 0 \\ 0 & \frac{1}{\alpha} \end{bmatrix} [Q(x)^f] dx$$

Formulation of matrix $[K^0]^e$

$$[K^0]^e = \hat{D}_b \times \int_0^L \begin{bmatrix} 0 & 0 \\ 0 & 0 \\ -1 & 0 \\ -2x & -\alpha \\ (-3x^2 + 6\alpha) & 0 \\ (-4x^3 + 18\alpha x) & 0 \end{bmatrix} \begin{bmatrix} 1 & 0 \\ 0 & \frac{1}{\alpha} \end{bmatrix} \begin{bmatrix} 0 & 0 & -1 & -2x & (-3x^2 + 6\alpha) & (-4x^3 + 18\alpha x) \\ 0 & 0 & 0 & -\alpha & 0 & 0 \end{bmatrix} dx$$

Before integration

$$[K^0]^e = \hat{D}_b \times \begin{bmatrix} 0 & 0 & 0 & 0 & 0 & 0 \\ 0 & 0 & 0 & 0 & 0 & 0 \\ 0 & 0 & 1 & 2x & (3x^2 + 6\alpha) & (4x^3 - 18\alpha x) \\ 0 & 0 & 2x & (4x^2 + \alpha) & (6x^3 - 12\alpha x) & (8x^4 - 36\alpha x^2) \\ 0 & 0 & (3x^2 - 6\alpha) & (6x^3 - 12\alpha x) & (9x^4 - 36\alpha x^2 + 36\alpha^2) & (12x^5 - 78\alpha x^3 + 108\alpha^2 x) \\ 0 & 0 & (4x^3 - 18\alpha x) & (8x^4 - 36\alpha x^2) & (12x^5 - 78\alpha x^3 + 108\alpha^2 x) & (16x^6 - 144\alpha x^4 + 324\alpha^2 x^2) \end{bmatrix}$$

After integration

$$[K^0]^e = \hat{D}_b \times \begin{bmatrix} 0 & 0 & 0 & 0 & 0 & 0 \\ 0 & 0 & 0 & 0 & 0 & 0 \\ 0 & 0 & L & L^2 & (L^3 - 6\alpha L) & (L^4 - 9\alpha L^2) \\ 0 & 0 & L^2 & \left(\frac{4}{3}L^3 + \alpha L\right) & \left(\frac{3}{2}L^4 - 6\alpha L^2\right) & \left(\frac{8}{5}L^5 - 12\alpha L^3\right) \\ 0 & 0 & (L^3 - 6\alpha L) & \left(\frac{3}{2}L^4 - 6\alpha L^2\right) & \left(\frac{9}{5}L^5 - 12\alpha L^3 + 36\alpha^2 L\right) & \left(2L^6 - \frac{39}{2}\alpha L^4 + 54\alpha^2 L^2\right) \\ 0 & 0 & (L^4 - 9\alpha L^2) & \left(\frac{8}{5}L^5 - 12\alpha L^3\right) & \left(2L^6 - \frac{39}{2}\alpha L^4 + 54\alpha^2 L^2\right) & \left(\frac{16}{7}L^7 - \frac{144}{5}\alpha L^5 + 108\alpha^2 L^3\right) \end{bmatrix}$$

Formulation of matrix $[K_c^e]$

$$[K_c^e] = [A_m^{-1}]^T \left(\hat{D}_{ab} \times \int_0^L [Q(x)^m]^T [Q(x)^f] dx \right) \times [A_f]^{-1} = [A_m^{-1}]^T [K_0^c] [A_f]^{-1}$$

$$[K_0^c] = \hat{D}_{ab} \times \int_0^L [Q(x)^m]^T [Q(x)^f] dx$$

Before integration

$$[K_0^c] = \hat{D}_{ab} \times \begin{bmatrix} 0 & 0 & 0 & 0 & 0 & 0 \\ 0 & 0 & -1 & -2x & (-3x^2 + 6\alpha) & (-4x^3 + 18\alpha x) \\ 0 & 0 & -x & -2x^2 & (-3x^3 + 6x\alpha) & (-4x^4 + 18\alpha x^2) \end{bmatrix}$$

After integration

$$[K_0^c] = \hat{D}_{ab} \times \begin{bmatrix} 0 & 0 & 0 & 0 & 0 & 0 \\ 0 & 0 & -L & -L^2 & \left(-\frac{3L^3}{4} + 6\alpha L\right) & (-L^4 + 9\alpha L^2) \\ 0 & 0 & -\frac{L^2}{2} & -\frac{2L^3}{3} & \left(-\frac{3L^4}{4} + 3\alpha L^2\right) & \left(-\frac{4L^5}{5} + 6\alpha L^3\right) \end{bmatrix}$$

REFERENCES

- [1] Chakraborty A., Gopalakrishnan S., Reddy J.N., 2003, A new beam finite element for the analysis of functionally graded materials, *International Journal of Mechanics Science* **45**(3): 519-539.
- [2] Kadoli R., Akhtar K., Ganesan N., 2008, Static analysis of functionally graded beams using higher order shear deformation theory, *Applied Mathematical Modeling* **32**(12): 2509-2525.
- [3] Kapuria S., Bhattacharyya M., Kumar A.N., 2008, Bending and free vibration response of layered functionally graded beams: A theoretical model and its experimental validation, *Composite Structures* **82**(3): 390-402.
- [4] Pindera M-J., Dunn P., 1995, An evaluation of coupled microstructural approach for the analysis of functionally graded composites via the finite element method, *National Aeronautics and Space Administration NASA*, Contractor Report 195455.
- [5] Ziou H., Guenfoud H., Guenfoud M., 2016, Numerical modelling of a Timoshenko FGM beam using the finite element method, *International Journal of Structural Engineering* **7**(3): 239-261.
- [6] Nguyen D.K., Gan B.S., 2014, Large deflections of tapered functionally graded beams subjected to end forces, *Applied Mathematical Modeling* **38**(11-12): 3054-3066.
- [7] Nguyen D.K., 2013, Large displacement response of tapered cantilever beams made of axially functionally graded material, *Composites Part B: Engineering* **55**: 298-305.
- [8] Kutíš V., Murin J., Belak R., Paulech J., 2011, Beam element with spatial variation of material properties for multiphysics analysis of functionally graded materials, *Computers and Structures* **89**(11): 1192-1205.
- [9] Murin J., Kutíš V., 2002, 3D-beam element with continuous variation of the cross-sectional area, *Computers and Structures* **80**(3-4): 329-352.
- [10] Lazreg H., Ait Amar Meziane M., Abdelhak Z., Hassaine Daouadji T., Adda Bedia E.A., 2016, Static and dynamic behavior of FGM plate using a new first shear deformation plate theory, *Structural Engineering & Mechanics* **57**(1): 127-140.
- [11] Rezaiee-Pajand M., Masoodi A.R., Mokhtari M., 2018, Static analysis of functionally graded non-prismatic sandwich beams, *Advances in Computational Design* **3**(2): 165-190.
- [12] Benferhat R., Daouadji T.H., Adim B., 2016, A novel higher order shear deformation theory based on the neutral surface concept of FGM plate under transverse load, *Advances in Materials Research* **5**(2): 107-120.
- [13] Lazreg H., Nafissa Z., Fabrice B., 2019, An analytical solution for bending and free vibration responses of functionally graded beams with porosities: Effect of the micromechanical models, *Structural Engineering & Mechanics* **69**(2): 231-241.
- [14] Guenfoud H., Himeur M., Ziou H., Guenfoud M., 2018, The use of the strain approach to develop a new consistent triangular thin flat shell finite element with drilling rotation, *Structural Engineering & Mechanics* **68**(4): 385-398.
- [15] Alshorbagy A.E., Eltaher M.A., Mahmoud F.F., 2011, Free vibration characteristics of a functionally graded beam by finite element method, *Applied Mathematical Modelling* **35**: 412-425.
- [16] Eltaher M.A., Samir A.E., Mahmoud F.F., 2012, Free vibration analysis of functionally graded size-dependent nano-beams, *Applied Mathematics and Computation* **218**: 7406-7420.
- [17] Eltaher M.A., Samir A.E., Mahmoud F.F., 2013, Static and stability analysis of nonlocal functionally graded nano-beams, *Composite Structures* **96**: 82-88.
- [18] Mahmoud F.F., Eltaher M.A., Alshorbagy A.E., Meletis E.I., 2012, Static analysis of nano-beams including surface effects by nonlocal finite element, *Journal of Mechanical Science and Technology* **26**(11): 3555-3563.
- [19] Hamed M.A., Eltaher M.A., Sadoun A.M., Almitani K.H., 2016, Free vibration of symmetric and sigmoid of functionally graded nano-beams, *Applied Physics A* **122**(9): 829.
- [20] Li X.F., Wang B.L., Han J.C., 2010, A higher-order theory for static and dynamic analyses of functionally graded beams, *Archive of Applied Mechanics* **80**(10): 1197-1212.